Properties of Green $SrAl_2O_4$ Phosphor in LDPE and PMMA Polymers

D.B. Bem,[1] H.C. Swart,[2] A.S. Luyt,[3] E. Coetzee,[2] F.B. Dejene[1]

[1]*Departmemnt of Physics, University of the Free State (Qwaqwa Campus), Phuthaditjhaba 9866, South Africa*
[2]*Departmemnt of Physics, University of the Free State, Bloemfontein 9300, South Africa*
[3]*Departmemnt of Chemistry, University of the Free State (Qwaqwa Campus), Phuthaditjhaba 9866, South Africa*

Received 3 February 2009; accepted 20 May 2009
DOI 10.1002/app.31405
Published online 27 April 2010 in Wiley InterScience (www.interscience.wiley.com).

ABSTRACT: Different contents of $SrAl_2O_4$:Eu,Dy, one of the long afterglow phosphorescent materials with high brightness, were melt-mixed with low-density polyethylene (LDPE) and Polymethyl methacrylate (PMMA) polymers, respectively. The morphology and composition of the samples were observed by means of a scanning electron microscope (SEM) coupled with an energy dispersive spectrometer (EDS), X-ray diffractometer (XRD), and transmission electron microscope (TEM). Sharp and broad X-ray diffraction (XRD) peaks were observed for the LDPE and the PMMA composites respectively, reflecting configuration characteristics similar to those of the respective pure polymers. TEM micrographs show a transition from nanosized particles to cluster formation with increase in phosphor concentration. The green long-lasting phosphorescence of the composites was observed in the dark after removal of the excitation light. Photoluminescence (PL) was observed in the composites of both polymers for phosphor volume concentrations above 1.0% for PMMA and above 0.5% for LDPE. For each of these samples, a broad PL peak at about 505 nm wavelength was observed after excitation at 350 nm with a xenon lamp. For the LDPE composites, the DSC results show that the presence of the phosphor in the polymer has no major influence on either the melting temperature or enthalpy values of the polymer. © 2010 Wiley Periodicals, Inc. J Appl Polym Sci 117: 2635–2640, 2010

Key words: LDPE-$SrAl_2O_4$:Eu,Dy composites; PMMA-$SrAl_2O_4$:Eu,Dy composites; luminescence; differential scanning calorimetry; thermogravimetric analysis

INTRODUCTION

The recognition of the size-dependence of the physical properties of materials has led to vigorous exploration of nanophase materials.[1–4] Nanophase materials are materials in the 1 to 100 nm range and exhibit greatly altered properties compared to their normal, large-grained counterparts with the same chemical composition. Phosphors constitute one of the categories of materials that show promising properties when synthesized in the nanophase. Strontium aluminate ($SrAl_2O_4$) is a solid, odorless, nonflammable pale yellow powder. It is chemically and biologically inert. When activated with a suitable dopant, e.g. europium, it acts as a photoluminescent material with long persistence of phosphorescence. Europium-activated strontium aluminate is a vastly superior phosphor than its predecessor, copper-activated zinc sulphide; it is about 10 times brighter, 10 times longer glowing, but 10 times more expensive than ZnS:Cu. The material is very hard, causing abrasion to machinery handling it; coating the particles with a suitable lubricant is usually used when strontium aluminate is added to plastics.

These phosphors find a wide range of applications such as in defence, domestic, commercial as well as in the scientific domains. These include use in luminous paints, as safety indicators in emergency cases, and in display devices (e.g. field emission displays and toys). Green emitting $SrAl_2O_4$ phosphors co-doped with europium (Eu) and dysprosium (Dy) have been focused on as high brightness and long afterglow characteristic materials.

Various mechanisms have been developed in an effort to explain the trapping and detrapping mechanisms in these materials. A mechanism based on hole trapping created by Dy^{3+} ions codoped into the host was developed on the long afterglow characteristics.[2–5] On the basis of some incompleteness in the prediction of certain experimental and theoretical phenomena, Clabau et al.[6] have more recently proposed a model of phosphorescence in terms of trapping of electrons only. Phosphor nano-composites can potentially be used to produce low-energy consumption and high-efficiency illumination for long hours. Progress in each of these areas depends on the ability to selectively and controllably deposit

Correspondence to: F.B. Dejene (dejenebf@qwa.ufs.ac.za).
Contract grant sponsors: The National Research Foundation, The University of the Free State in South Africa.

nano-particles, and to uniformly disperse the phosphors in the host matrix, to create a strong and stable three dimensional network. Though rare-earth ion-doped alkaline earth aluminate phosphors have been extensively investigated,[1,7,8] there is a lack of work done on phosphor hosts, particularly for outdoor applications, an area that finds increasing use for these materials. Exposure to moisture and other environmental factors have the potential to cause accelerated degradation in luminance.

In this article, the mixing conditions, luminescence as well as thermal properties of the newly developed $SrAl_2O_4:Eu^{2+},Dy^{3+}$ phosphor introduced into two polymer matrices, low-density polyethylene (LDPE) and polymethyl methacrylate (PMMA), is reported. The characterized properties are also discussed. The lower density of polymers, compared to metals and ceramics, as well as resistance to atmospheric and other forms of corrosion, render them more suitable for these applications. Some semicrystalline polymers are known to undergo strain-related deformations that are likely to facilitate the occurrence of phosphorescence, hence the choice of LDPE. The amorphous PMMA was used as a control parameter. In addition, the two polymers are readily available and environmentally stable.

EXPERIMENTAL

Materials

Commercially produced strontium aluminate powder from Phosphor Technology in the UK was used. It has a density of 3.67 g cm^{-3} and a melting point of 1200°C. PMMA has a melt flow index (MFI) of 0.8 g/10 min, a melting point of 135°C, and a density of 1.19 g cm^{-3}. LDPE has an MFI of 2.0 g/10 min, a melting point of 110°C, and a density of 0.922 g cm^{-3}. The polymers were supplied by Sasol Polymers, South Africa.

Sample preparation

The preparation of $SrAl_2O_4$:Eu phosphor has already been reported elsewhere.[9,10] Polymer-phosphor composites were produced by melt-mixing the green emitting $SrAl_2O_4$ phosphor into low-density polyethylene (LDPE) and polymethyl methacrylate (PMMA), respectively, at volume ratios ranging from 0.05% to 5%. Samples were weighed according to the required ratios and mixed using a volume of 50 cm^3 in a Brabender Plastograph (Brabender OHG-DUISBURG Kulturs 51-55) mixing chamber at a screw speed of 30 rpm for 15 min. The mixing was carried out at 160°C and 180°C for LDPE and PMMA, respectively. The samples, whose average thickness was 0.43 ± 0.08 mm, were extruded at 200°C and 250°C for LDPE and PMMA, respectively.

Morphology and structural analysis

The microstructure and elemental composition of the samples were investigated using a scanning electron microscope (SEM) (Shimadzu model ZU SSX – 550 Superscan) coupled with an energy dispersive X-ray spectrometer (EDS). The as-prepared samples were directly cut into pieces of appropriate sizes. Before the SEM analyses and EDS measurements, the samples were mounted on aluminum stubs with conductive double sticking carbon tape and gold-sputter-coated to facilitate electron conduction. The morphology and particle size of the composites were observed by transmission electron microscopy (TEM). TEM images were recorded on a JEOL-JEM 200CX transmission electron microscope. To study the crystalline/amorphous structures of the products, XRD measurements were carried out at room temperature. XRD scans of the samples were performed with a Bruker AXS Discover diffractometer with CuK_α radiation of wavelength 1.5418 Å.

Photoluminescence (PL) measurements

PL measurements were made on a Carry Eclipse Fluorescence Spectrophotometer system, equipped with a 150 W xenon lamp as the excitation source. Samples were excited at 350 nm and emission observed in the wavelength range 400 to 600 nm at room temperature.

Thermal analysis

A Perkin-Elmer DSC 7 differential scanning calorimeter, under flowing nitrogen, was employed for the DSC analyses. The system was interfaced to a computer, which was used for calculations by means of the Pyris software. Calibration of the system was based on the onset temperatures of melting of indium and zinc standards, as well as the melting enthalpy of indium. Samples of masses ranging from 7 to 10 mg were sealed in aluminum pans and heated from 25 to 160°C at a heating rate of 10°C min^{-1}, and immediately cooled at the same rate to 25°C. For the second scan, the samples were heated and cooled under the same conditions. Peak temperatures of melting and crystallization, as well as melting and crystallization enthalpies, were determined from the second scan. Thermogravimetric analyses (TGA) were performed in a Perkin-Elmer TGA7 thermogravimetric analyzer in a flowing nitrogen atmosphere (flow rate 20 mL min^{-1}). The samples, each having a mass between 6 and 10 mg, were heated from 25 to 600°C at a rate of 10 °Cmin^{-1}. For

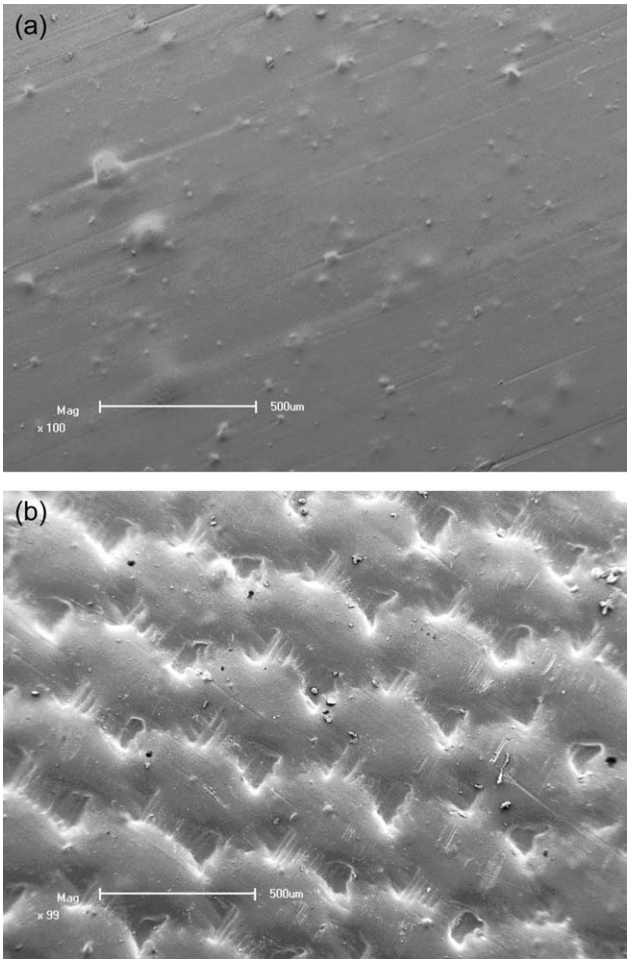

Figure 1 SEM images of (a) 97/3 v/v LDPE/phosphor [×100 magnification], (b) 97/3 v/v PMMA/phosphor [×100 magnification], and (c) 97/3 v/v PMMA/phosphor [×400 magnification].

both DSC and TGA analyses three measurements were performed on each sample composition, from which average temperature and enthalpy values were calculated.

RESULTS AND DISCUSSION

Figure 1 shows the SEM micrographs of the polymer composites. Two types of morphology can be observed. The first consists of large and small particles (lumps) superimposed on an otherwise smooth surface [Fig. 1(a)]. Most probably, these lumps are nondispersed phosphor particles. However, EDS point analysis confirmed the distribution of phosphor particles throughout the whole polymer surface for the different concentrations. The second type of morphology observed consists of leaflet-like structures [Fig. 1(b)]. Based on available results, these patterns are most probably the result of the mechanical sample manufacturing process. The EDS results, shown in Figure 2, show the presence of the expected elements, i.e., strontium, aluminum, oxygen, and carbon. It is found that for each of the respective phosphor concentrations, the distribution of the elements, strontium, aluminum, and oxygen, in the polymer matrices, is fairly uniform.

Typical XRD patterns recorded for the composites of LDPE and PMMA are displayed in Figure 3. The $SrAl_2O_4$ crystal is characterized by planes having diffraction peaks of (011), (020), (−211), (220), (211), (031), and (400). The measurements displayed here have visible peaks at 20°, 30°, and 35°, corresponding to the planes (020), (220), and (031). The (020) and (031) peaks indicate the presence of $SrAl_2O_4$. The absence of the expected phosphor peaks in the XRD spectra may be due to the low concentration of the phosphor in the polymer matrix. It is observed that as the phosphor concentration in LDPE increases, there are no changes in the peak positions. These results indicate that the introduction of the phosphor did not significantly change the general structure of the polymer. Particle sizes calculated from Scherrer's equation have a wide range, but in the nanometer range, averaging 70 ± 23 nm.

Figure 4 shows the TEM micrograph of the 5% phosphor containing PMMA composite. The image shows the basic morphology of the phosphor particles and their distribution at the low phosphor concentration. The particles are fairly monodisperse in size and isotropic in shape.

The LDPE composites with a phosphor concentration greater than 0.5% and PMMA composites with a concentration greater than 1.0% show an intense green emission, as shown in Figure 5. The PL spectrum corresponding to each concentration is composed of a broad PL band peaking near 510 nm. This green photoluminescence has been attributed to

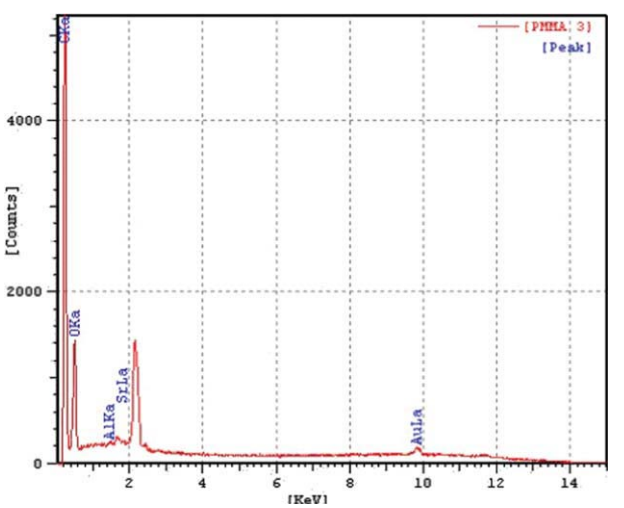

Figure 2 Point EDX results of 97/3 v/v LDPE/phosphor. [Color figure can be viewed in the online issue, which is available at www.interscience.wiley.com.]

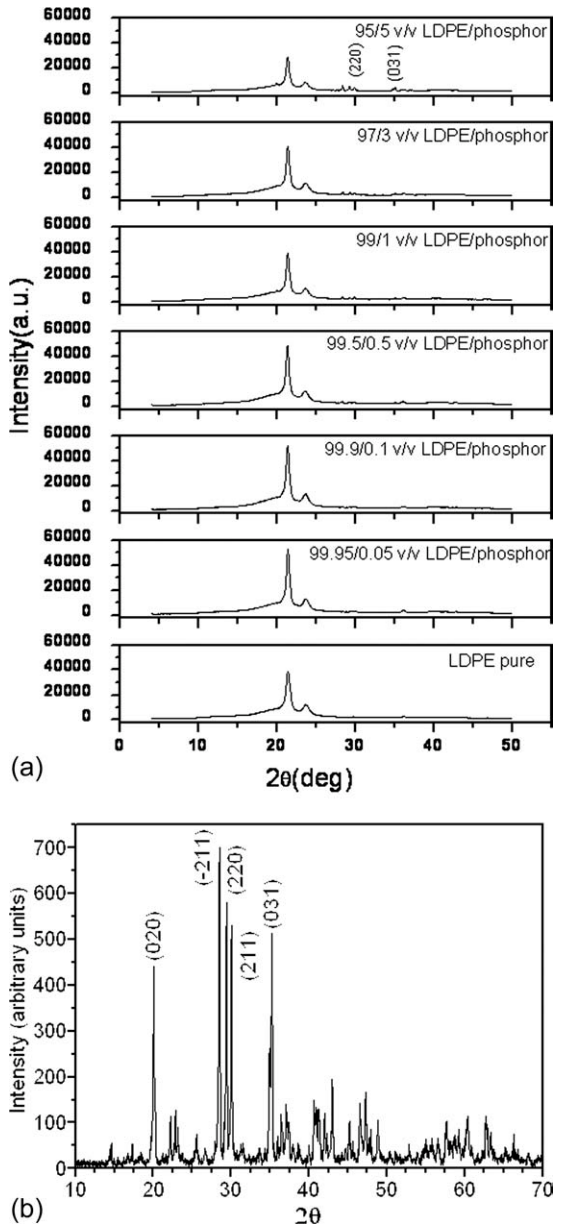

Figure 3 XRD spectra of (a) LDPE composites and (b) green-emitting $SrAl_2O_4:Eu^{2+}Dy^{3+}$- phosphor.

the $4f^65d^1 \rightarrow 4f^7$ electronic transition of the divalent europium ion (Eu^{2+}) in the $SrAl_2O_4:Eu^{2+}$ bulk phosphors, as reported earlier.[2,3] The PL peaks for LDPE shift to higher wavelengths with increasing phosphor concentration. Higher phosphor concentration favors the excitation of the green luminescence wavelength (520 nm) which is attributed to the Eu^{2+} emission center.

Figure 6 correlates the photoluminescence intensity with the phosphor concentration. The superiority in luminescence displayed by LDPE is probably a consequence of a polaronic effect in which phosphor particles may be responsible for an alternation in the polymer bond geometry, giving rise to the creation of an "excited state" (polaron), which on being

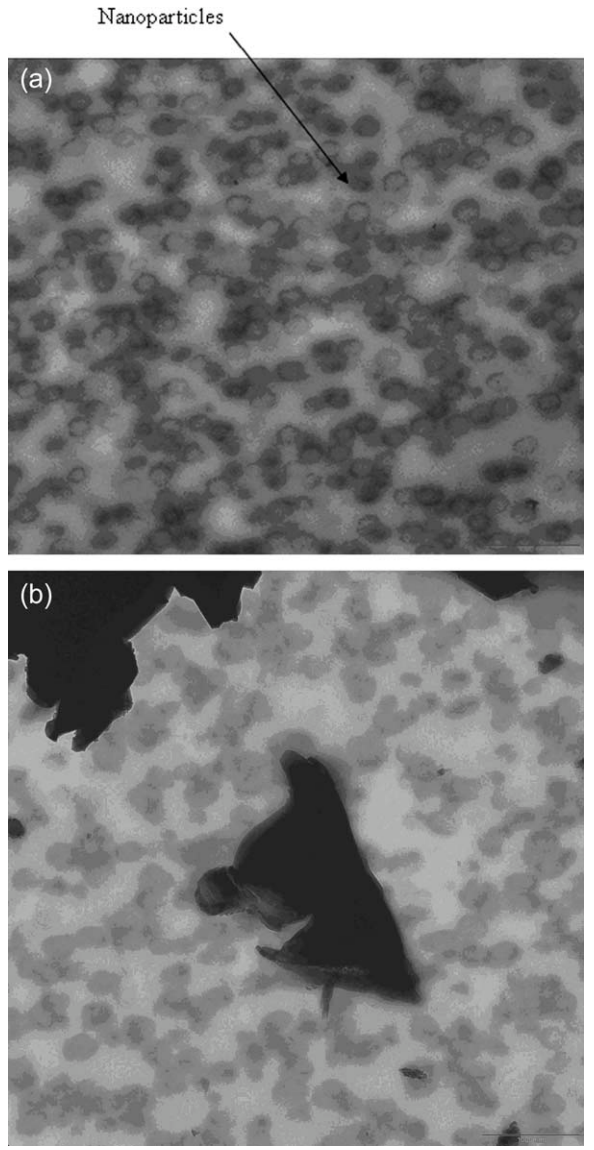

Figure 4 (a) TEM micrograph of 0.5% phosphor in PMMA (b) TEM micrograph of 5% phosphor in PMMA.

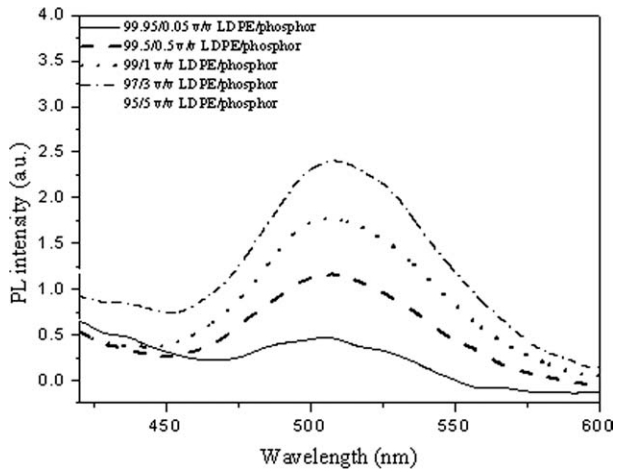

Figure 5 PL spectra for pure LDPE and the 5% phosphor containing composite.

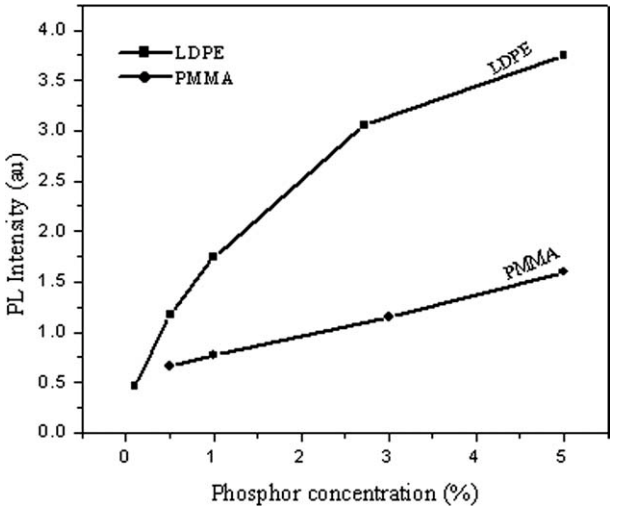

Figure 6 Concentration-dependence of the luminescence of the composites.

relaxed may lead to the energy being emitted radiatively.

The DSC curves for LDPE and its composites are shown in Figure 7. The average values of the peak temperatures of melting, as well as the melting and crystallization enthalpy values, are summarized in Table I. The heating curves in Figure 7(a) show endothermic peaks at about 112°C, with no significant peak shifts, suggesting that the phosphor content did not have an appreciable effect on the melting temperature of LDPE. The comparison between the observed and expected enthalpies (calculated taking into account the weight fraction of LDPE in the samples, and assuming that the LDPE crystallization mechanism does not change in the presence of the phosphor particles) shows lower than expected enthalpies for the composites at low phosphor contents, but at higher phosphor concentrations the experimentally observed enthalpies are higher. This behavior may be explained by the fact that the particles are not agglomerated at low contents, and therefore there are large interfacial areas between the nano-particles and the polymer. This will result in immobilization of the polymer chains and accompanying decrease in crystallinity. At high phosphor

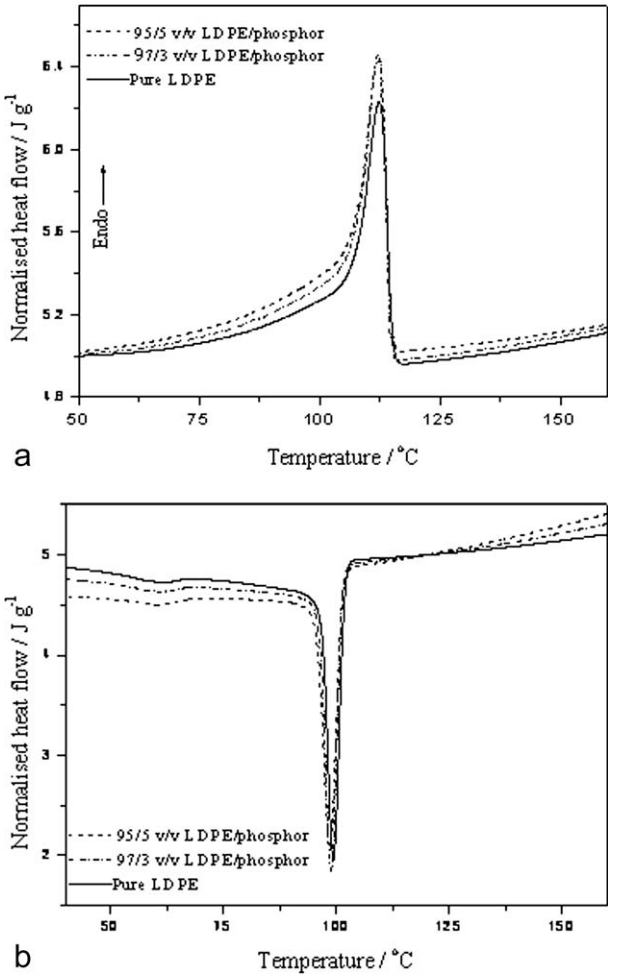

Figure 7 DSC (a) heating and (b) cooling curves of LDPE and its phosphor composites.

contents there is particle agglomeration, which probably gives rise to epitaxial crystallization of LDPE on the phosphor surfaces.[11]

The TGA results, Figure 8, show that the composites start decomposing at higher temperatures than pure LDPE. The main degradation for the pure polymer starts at about 380°C and leaves a residue at 496°C, while the corresponding values for the composites are 402°C and 501°C, respectively. This indicates that the phosphor particles increased the

TABLE I
DSC Data of LDPE and its Phosphor Composites

Vol % phosphor	T_m (°C)	ΔH_m^{obs} (J g^{-1})	ΔH_m^{cal} (J g^{-1})	T_c (°C)	ΔH_m^{obs} (J g^{-1})	ΔH_c^{cal} (J g^{-1})
0.00	112.5 ± 0.3	80.7 ± 6.4	–	99.1 ± 0.1	−61.8 ± 4.5	–
0.05	112.5 ± 0.4	62.7 ± 2.0	80.5	99.2 ± 0.1	−52.9 ± 2.2	−61.7
0.10	112.3 ± 0.3	76. 6 ± 2.1	80.4	99.2 ± 0.4	−56.7 ± 2.7	−61.6
0.50	112.1 ± 0.0	72.2 ± 6.0	79.2	98.8 ± 0.0	−55.1 ± 6.7	−60.6
1.00	112.4 ± 0.2	70.6 ± 0.3	77.6	98.7 ± 0.1	−58.8 ± 3.5	−59.3
3.00	112.2 ± 0.6	75.5 ± 0.2	72.1	98.7 ± 0.2	−58.7 ± 6.4	−55.0
5.00	112.3 ± 0.3	75.9 ± 0.3	67.4	98.7 ± 0.9	−54.2 ± 4.3	−51.3

ΔH_m and ΔH_c, melting and crystallization enthalpies; T_m and T_c, peak temperatures of melting and crystallization.

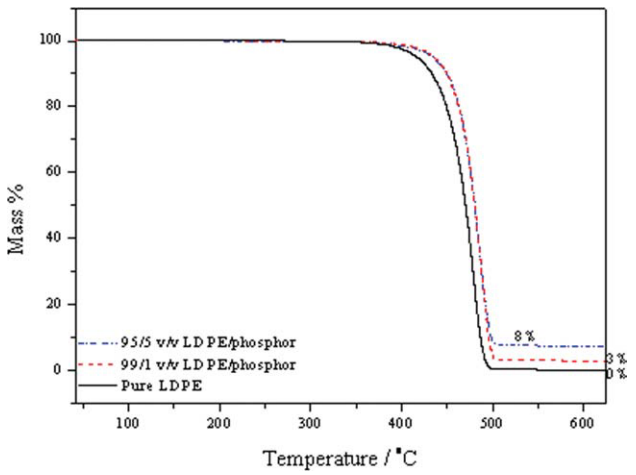

Figure 8 TGA curves for LDPE and its composites. [Color figure can be viewed in the online issue, which is available at www.interscience.wiley.com.]

thermal stability of the polymer, but that the rates of degradation are higher than that of pure LDPE. The residual mass corresponds to the amount of phosphor initially mixed with the polymer. An observation similar to this, made for LDPE-copper composites,[12] was attributed to the relatively higher heat capacity and thermal conductivity values of copper, which caused it to preferentially absorb the heat. In view of the higher values of the heat capacities and thermal conductivities for ceramics, the increased stability in the LDPE-phosphor composites may be explained in a similar way. However, extended heat absorption by the phosphor particles, may cause these particles to reach a higher temperature than the surrounding matrix resulting in a more rapid degradation of the polymer. Alternatively, the phosphor particles may temporarily trap the volatile degradation products, which will escape at a faster rate as soon as they acquire enough energy at higher temperatures.

CONCLUSIONS

This study has provided some insight into the ability to controllably mix nano to microsized phosphor particles into and to uniformly disperse them in both semi-crystalline and amorphous polymer matrices. To elucidate this information, the morphology, photoluminescence, and thermal properties of the polymer composites were investigated. SEM micrographs and EDS spectra showed generally smooth morphologies and a fairly uniform distribution of phosphor particles in the polymer matrices. XRD peaks for the composites of the polymers are similar to those of the pure polymers, manifesting a close resemblance in the configurations of the pure polymers and their phosphor composites. TEM micrographs reveal monodispersed, nanosized phosphor particles. A characteristic green emission peak at about 505 nm wavelength was exhibited by the composites. Peak intensities of the PL emission spectra monotonously increased with an increase in phosphor concentration. The higher intensity values in LDPE are probably due to a polaronic effect. The DSC results for LDPE do not show a major influence of the phosphor content on either the melting temperature or enthalpy of the polymer. These results demonstrate that LDPE can be employed to create a suitable three-dimensional phosphor network for practical luminescence applications.

Special appreciation goes to Ms. Julia Mofokeng who assisted with sample preparation as well as thermal measurements.

References

1. Murayama, Y.; Takeuchi, N.; Aoki, Y.; Matsuzawa, T. U.S. Pat. 5,424 (1995).
2. Matsuzawa, T.; Aoki, Y.; Takeuchi, N.; Murayama, Y. J Electrochem Soc 1996, 143, 2670.
3. Katsumata, T.; Sakai, R.; Komuro, V.; Morikawa, T. J Electrochem Soc 2003, 150, H111.
4. Qiu, J.; Gaeta, V.; Hirao, V. Chem Phys Lett 2001, 333, 236.
5. Katsumata, T.; Sakai, R.; Komuro, S.; Morikawa, T.; Kimura, H. J Cryst Growth 1999, 198, 869.
6. Clabau, F.; Rocquefelte, X.; Jobic, S.; Deniard, P.; Whangbo, M. H.; Garcia, A.; Mercier, T. L. Chem Mater 2005, 17, 3909.
7. Shionoya, S.; Yen, W. M., Eds. Phosphor Handbook; CRC Press: Boca Raton, FL, USA, 1999; p 651.
8. Nakamura, T.; Kaiya, K.; Takahashi, N.; Matsuzawa, T.; Rowlands, C. C.; Beltran-Lopez, V.; Smith, G. M.; Riedi, P. C. J Mater Chem 2000, 10, 2566.
9. Tsutai, H.; Shimizu, I.; Kawakami, T.; Shinbo, K.; Kato, K.; Kaneko, F. M. Tech Rep IEICE CPM 1995, 13, 95.
10. Tsutai, T.; Kamimura, I.; Kato, K.; Kaneko, F.; Shinbo, K.; Ohta, M.; Kawakami, T. Tech Rep IEICE CPM 1997, 55, 97.
11. Mbhele, Z. H. G.; Salemane, M. G.; Sittert, C. E.; Nedeljkovi, J. M.; Djokovic, V.; Luyt, A. S. Chem Mater 2003, 15, 5019.
12. Luyt, A. S.; Molefi, J. A.; Krump, H. Polym Degrad Stab 2006, 91, 1629.